Lysergic acid diethylamide pretreatment prolongs brain-stimulation induced neural activity

Lucas L. Dwiel[a], Mackenzi L. Prina[b], Elise M. Bragg[a], Matthew Company[c], Lucky L. Drucker[d], Laetitia R. Reduron[e], Bryan W. Luikart[b], Wilder T. Doucette[a,f]

a Department of Psychiatry, Dartmouth Hitchcock Medical Center, Lebanon NH

b Department of Neurobiology, Heersink School of Medicine, University of Alabama at Birmingham, Birmingham AL

c Integrative Neuroscience at Dartmouth, Guarini School of Graduate and Advanced Studies, Dartmouth College, Hanover NH

d Department of Molecular and Systems Biology, Geisel School of Medicine, Dartmouth College, Hanover NH

e Molecular & Cellular Biology, Guarini School of Graduate and Advanced Studies, Dartmouth College, Hanover NH

f Geisel School of Medicine at Dartmouth, Dartmouth College, Hanover NH

Abstract

A leading theory for how psychedelics are able to produce robust clinical improvement and preclinical behavioral changes is that psychedelics act through neuroplastic mechanisms to induce lasting structural and functional alterations in neural circuits. However, psychedelics produce these effects across wide swaths of the brain. Based on our prior work, we hypothesized that engaging a specific brain circuit with focal brain stimulation during the window of enhanced plasticity produced by psychedelics would lead to more persistent alterations in the activity of that circuit. To test this, we administered either saline (SAL) or lysergic acid diethylamide (LSD) to rats 24 hours prior to electrical stimulation targeting the rat medial prefrontal cortex (mPFC). Brain activity was recorded before, during, and after stimulation using depth electrodes implanted in four bilateral frontostriatal regions.

To assess changes in neural activity, we trained general logistic classifiers to distinguish between time points (e.g., pre-stimulation vs. post-stimulation) and then compared model performances across groups (e.g., LSD vs. SAL). As such, model performance represents the degree of difference between the two neural states (pre vs. post), and a significant difference between groups indicates a larger change in brain activity in one group. We found that LSD pretreatment, compared to SAL, resulted in larger and longer-lasting changes in brain activity following stimulation. Immunohistochemistry revealed that stimulation led to the activation of the mTOR signaling pathway, and the combination of LSD and stimulation led to alterations in perineuronal net (PNN) integrity. Regardless of pretreatment, brain activity states recorded during stimulation did not capture

the brain state that persisted in the minutes or days that followed. This work has important implications for understanding the general effects of brain stimulation and provides strong support for the development of psychedelic-assisted brain stimulation approaches. By increasing the durability of brain stimulation-induced changes in activity, this approach could lead to a reduction in relapse rates, which currently limit the impact of non-invasive stimulation treatments.

Introduction

Psychedelics have garnered considerable interest in the treatment of multiple psychiatric disorders with a small number of doses, sometimes a single dose, leading to significant alterations in mindset and behavior for months.[1–5] A leading hypothesis for this longevity is that psychedelics alter neural plasticity, allowing for long-lasting structural and functional changes in the brain. The biomolecular pathways by which psychedelics engage neuroplastic processes are complex; however, many of these pathways converge on mammalian target of rapamycin (mTOR), a kinase that regulates cell growth, protein synthesis, and transcription. Not only do psychedelics upregulate mTOR activation [6,7], but mTOR antagonists block the effects of psychedelics on dendritic growth [8,9], neural firing rate [10], and behavior [10]. Brain stimulation alone has also been shown to impact neuroplasticity, and this effect may be mediated through mTOR activation [11–13]. Therefore, mTOR serves as a possible point of convergence of psychedelics and brain stimulation in mediating neuroplasticity.

Although non-invasive brain stimulation can have robust acute effects, these effects typically do not last, leading to depression relapse rates as high as 80% within 6 months [14–17], anxiety relapse of 50% within 3 months [18], and mixed effects in post-traumatic stress disorder (PTSD) with some reporting degradation of clinical effect within 2 months [19] and others seeing stability out to 3 months [20]. Historically, this has meant that stimulation protocols were lengthened, and/or patients would periodically come back to the clinic for additional stimulation sessions. Recent accelerated protocols, like the Stanford Neuromodulation Therapy (SNT; previously SAINT) for transcranial magnetic stimulation (TMS), have condensed these multi-week stimulation sessions into a 5 day protocol producing decreased depression for up to 4 weeks, but beginning to increase again in the fifth, and last week, of the study.[21] However, even in those who successfully remit with SNT, only 47% remain in remission 12 weeks later.[22] Besides altering the course of stimulation, there is also burgeoning evidence for pharmacological adjuvants targeting NMDA-dependent plasticity [23] being paired with transcranial magnetic stimulation to increase response rates and produce larger decreases in depressive symptoms out to 4 weeks [24]. Although exciting, it remains to be seen how persistent and replicable these newer stimulation protocols will be when implemented more broadly.

The rodent IL target was selected due to its homology to the human subcallosal cingulate, which is an established target of stimulation for depression in patients and in pre-clinical depression models. We have already shown that infralimbic cortex (IL) brain stimulation 24 hours after LSD administration can lead to larger and distinguishable changes in brain activity compared to stimulation following saline (SAL) [25]. Based on these results and what is known about the effects of psychedelics on neuroplasticity, we hypothesized that LSD would allow stimulation to produce longer lasting changes in brain activity. Therefore, we pretreated rats with either SAL or LSD, waited 24 hours, stimulated the IL, and quantified changes in local field potentials (LFPs) during and immediately after stimulation, and during 30 minute sessions for 7 days following stimulation. Given mTOR's potential role as a point of convergence between stimulation- and

psychedelic-mediated plasticity, and given the role of perineuronal nets (PNNs) in governing neuroplasticity[26,27], we performed immunofluorescence staining in one cohort of rats the day of stimulation to assess mTOR activation and PNN integrity.

Methods

Cohorts

We used three cohorts of Sprague-Dawley rats (Charles River; Shrewsbury, MA) for these experiments. All rats arrived at 60 days old. The first cohort had 7 rats (3 female and 4 male; 124-125 days old). The second cohort had 10 rats (4 female and 6 male; 116-388 days old). The third cohort had 21 rats (10 female and 11 male; 141-496 days old) including 6 rats that had been trained on a delay discounting task for a separate experiment and we waited at least 1 month before using them in this experiment.

Drugs

We delivered 0.2 mg/kg LSD (Sigma Aldrich) via an intraperitoneal injection mixed with sterile SAL. We injected SAL at the same volume as LSD.

Electrode implantation

We anesthetized rats using an isoflurane/oxygen mixture (5% isoflurane for induction and 2% for maintenance) and stereotactically implanted them with custom electrode arrays[28] to record LFPs and deliver electrical stimulation. Briefly, these electrodes use a custom milled plastic base with polyimide tubing that guides two wires to each brain location (one nichrome wire for recording, 50 µm diameter, and the other stainless steel wire for stimulating, 125 µm). We implanted the electrodes with the plastic base attached to the skull surface with acrylic cement. All electrodes targeted bilateral mPFC/infralimbic cortex (IL; AP 3.4 mm; ML ±0.75 mm; and DV -5.0 mm), orbitofrontal cortex (OFC; AP 3.4 mm; ML ±3.0 mm; and DV -6.0 mm), nucleus accumbens shell (NAcS; AP 1.2 mm; ML ±1.0; and DV -7.6 mm), and nucleus accumbens core (NAcC; AP 1.2 mm; ML ±2.4 mm; and DV -7.6 mm). All coordinates are relative to bregma.

Stimulation

We used a Plexon stimulator (PlexStim, Plexon; Plano, TX) to deliver clinically based stimulation parameters (biphasic, 130 Hz, 90 µs pulse width, and ±200 µA) targeting bilateral IL. To obtain artifact-free LFPs during stimulation, every 50 seconds we turned the stimulation off for 10 seconds, repeating this either 60 or 120 times for 1 to 2 hours respectively; cohort 1 and 3 received 1 hour of stimulation, cohort 2 received 2 hours of stim. We verified current and voltage of stimulation before and after each session with a factory-calibrated oscilloscope (TPS2002C, Tektronix; Beaverton, OH). For sham stimulation, we plugged the rats in with the same stimulation cable, but did not pass any current.

Local field potential recording and processing

We recorded LFPs from freely-moving rats using a Plexon Omniplex digital acquisition system including commutators integrated into sound-proof enclosures (MedAssociates; Fairfax, VT) and simultaneous video

acquisition using Plexon's Cineplex system. We recorded LFPs at 20 kHz, downsampled the data to 2000 Hz, and applied a type I Chebyshev notch filter to remove 60 Hz line noise. We quantified LFP features within 3-second windows with 50% overlap and removed any windows that had noise artifacts as defined by raw signals above or below ±2 mV or fell within an active stimulation interval. Within the clean 3-second windows, we calculated power using *pwelch()* and calculated imaginary coherence by taking the imaginary component of the output of *cmtm()* which uses a multi-taper method [29] across six frequency ranges: delta (Δ) = 1-4 Hz, theta (θ) = 5-10 Hz, alpha (α) = 11-14 Hz, beta (β) = 15-30 Hz, low gamma (lγ) = 45-65 Hz, and high gamma (hγ) = 70-90 Hz. We used the imaginary component of coherence to minimize the influence of volume conduction and a common reference.[30] From the 8 recording locations (bilateral mPFC, OFC, NAcC, and NAcS) we obtained 48 power features and 168 coherence features, providing a total of 216 features to describe brain states.

Experimental design

In cohort 1, we injected each rat with SAL, waited 24 hours, collected 10 minutes of pre-stimulation LFPs, stimulated IL for 1 hour, collected post-stimulation LFPs for ~1 hour, and then collected 30 minutes of LFPs 1, 2, 3, 6, and 7 days after stimulation. We waited at least one week before injecting LSD and repeating the same recording schedule. In cohort 2, we injected each rat with SAL, waited 24 hours, collected 10 minutes of pre-stimulation LFPs, stimulated IL for 2 hours, collected post-stimulation LFPs for ~1 hour, and then collected 30 minutes of LFPs 1, 2, and 3 days after stimulation. We waited at least one week before injecting LSD and repeating the same recording schedule. In cohorts 1 and 2, we always administered LSD second to avoid any potential persisting effects of LSD paired with IL stimulation (LSD+sIL) confounding our SAL control. In cohort 3, we split the rats into 4 groups: SAL+sham (n = 5; 2 female, 3 male), SAL+sIL (n = 6; 3 female, 3 male), LSD+sham (n = 6; 2 female, 4 male), and LSD+sIL (n = 4; 3 female, 1 male). We injected each rat with either SAL or LSD, waited 24 hours, collected 10 minutes of pre-stimulation LFPs, stimulated IL for 1 hour, collected post-stimulation LFPs for ~20 minutes, and then euthanized the rats for mTOR and PNN staining (see mTOR/PNN below). Two rats, 1 male in SAL+sIL and 1 male in LSD+sham, did not contribute any neural data due to missing files. See **Fig. 1** for an experimental diagram of each cohort.

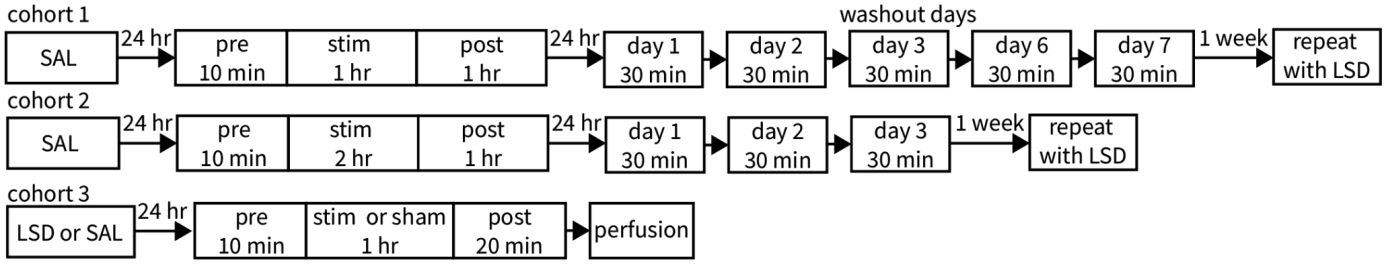

Fig. 1 Experimental flowchart for each cohort.

Model training and testing

To determine the effect of LSD on brain stimulation, we trained two kinds of logistic classifiers using *fitglm()* in Matlab (2025b; Natick, MA): 1. pre vs. post models we trained to differentiate between pre-stimulation LFPs and post-stimulation LFPs; 2. pre vs. stim models we trained to differentiate between pre-stimulation LFPs and LFPs from the clean recording intervals during stimulation; and 3. SAL vs. LSD models we trained to differentiate between SAL post and LSD post or SAL stim and LSD stim. For the first two model types, we built

separate models for the LSD and SAL data. In the third model type, we z-scored post and stim data by corresponding pre data. In all modeling, we subsampled or weighted our data such that each rat contributed the equivalent of 100 pre samples and 100 post samples (pre vs. post) or 100 pre samples and 100 stim samples (pre vs. stim). We then split each rat's data such that 80% was used for training and the remaining 20% was set aside for testing. Once we built the models, we tested each on the corresponding test set (post→post, P→P; stim→stim, S→S) and quantified performance as the area under the receiver operator characteristic curve (AUC) using *perfcurve()*. To account for variation due to subsampling, we repeated all model building and testing 100 times. To characterize the variability of model performance across the hour post stimulation and across rats, we split the data into 5 minute intervals. We then used the same models as above and tested each only on the data from a single rat during a given 5 minute interval. To characterize the persistence of brain activity changes, we also tested pre vs. post and pre vs. stim models on washout days by swapping the post/stim test data with washout data (P→wash and S→wash). To determine the similarity between LSD and SAL models, we cross-applied models such that we tested the LSD pre vs. post models on SAL pre vs. post data and vice versa (LSD→SAL and SAL→LSD). To compare pre vs. post models to pre vs. stim models, we tested LSD pre vs. stim models on LSD pre vs. post data and likewise for SAL data (stim→post, S→P). For single feature analysis, we used the exact same training and testing data, but built and tested individual models for each LFP feature. We built sex specific pre vs. post models to test for sex differences.

In a subset of rats from cohorts 1 and 2 (n = 14; 7 female and 7 male) we obtained LFP data before any injection to serve as a sham stimulation control (SHAM). By building these models the same way as above, we are able to account for model performance due to changes in LFPs not driven by an intervention (e.g., changes in signal quality through time and potential overfitting due to 80:20 modelling). For the first recording, we arbitrarily split the 30 minute recording into two halves to serve as pseudo 'pre' and 'post' data, built pre vs. post models as above, and then tested these models on left out data from the same recording and using subsequent recordings as our 'washout' post data on which to do testing. The washout data (24, 48, and 96 hours) did not perfectly match the data in the LSD or SAL groups (24, 48, 72, 144, and 196 hours) so we averaged performances across all washout days to obtain an estimate of SHAM model performance (AUC = 0.67±0.05; **Extended Data Figure 1**) — this performance is indicated as a dashed line in the appropriate figures. In addition to these sham models, we also built permuted models from the LSD and SAL data in which we shuffled the assignment of LFP training data to groups to obtain an estimate of by-chance model performance. Since our models are binomial classifications, these permuted models are always centered near an AUC of 0.5. All real models outperformed these permuted models which likely give an overly conservative null distribution. Therefore, we only visualized the permuted distributions when necessary. Likely, the true null distribution for the washout data falls between the fully permuted performances and the performance of the SHAM models, between 0.5 and 0.67.

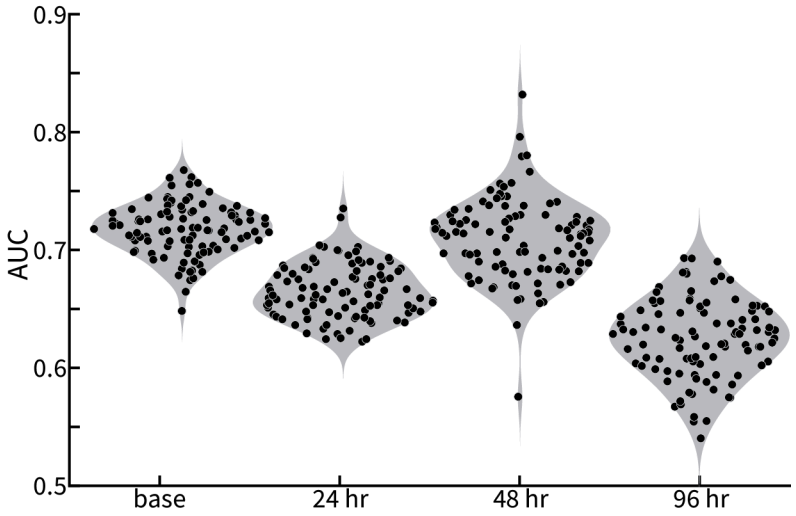

Extended Data Figure 1 Sham stimulation models built from recordings before any injections showing performance across time. We averaged performances on 24, 48, and 96 hours after the baseline data to provide an estimate of model performance on washout days due to non-interventional changes through time.

Model performance comparison

Permutation tests

When directly comparing the performance distributions of two models (e.g., comparing LSD pre vs. post model to its permuted version) we used permutation tests. Briefly, we used the formula p = (1+m)/(1+b) where m is the number of times that the permuted distribution outperformed the mean of the real distribution and b is the number of values in the permuted distribution [31].

Model performances through time

When comparing the performance distributions of models across time, we used linear mixed effects models using the following formula: AUC ~ Group*Time. Here, 'Group' could represent LSD, SAL, or permuted and 'Time' represents each washout day. We used post hoc permutation tests (see above) to determine which comparisons drove significant differences.

Variability across time and rats

To compare the variability of model performance across LSD and SAL groups, we calculated the standard deviation of AUCs per rat across each 5 minute post-stimulation interval (variability across time) and the standard deviation of AUCs per 5 minute post-stimulation interval across rats (variability across rat). We then compared these distributions of standard deviations between LSD and SAL using two-sample t-tests.

Feature visualization

To visualize individual LFP features across time, we z-scored feature values to their baseline levels and then averaged across rats either in 5 minute intervals for during and post-stimulation or across the 30 minute washout day recording.

Washout feature comparison

To determine which LFP features remained altered on the first washout day in the LSD group, we computed a 95% threshold from the corresponding permuted single features. We then compared this subset of features to the same features in the SAL group using a permutation test. We visualized any feature that both outperformed permuted and SAL performances. Last, we used *corrcoef()* to calculate the Pearson correlation coefficient of stim→stim single feature performances and stim→wash performances to determine if the same features differentiate both cases.

Velocity

We used DeepLabCut[32] for automated tracking of all videos. We trained our model on 82 videos, each with 20 hand-labeled frames. Of the 82 videos, 26 came from unimplanted rats and the remaining 56 came from implanted rats. We then used the position data of 4 body parts (tail base, spine center, shoulder center, and neck) to define a centroid, removing any data given a likelihood less than 80%. We then calculated the change in position of this centroid across each frame and obtained the total distance travelled for each minute, giving a velocity of pixels/minute. To determine if velocity alone could be used to differentiate between pre and post or pre and washout intervals we followed the same procedure as described for LFPs: building pre vs. post models of velocity and testing each on left-out data and data from washout days and building/testing permuted pre vs. post models.

mTOR/PNN

Immunohistochemistry

After collecting ~20 minutes of post-stimulation LFPs, we sacrificed and perfused the rats with PBS and 4% paraformaldehyde. We extracted the brains and stored them in 4% paraformaldehyde. We sliced the brains coronally with a Leica VT1000S vibratome at 65 µm. We permeabilized these sections for 30 minutes in PBS with 0.4% Triton-X (PBS-T) on a rocking platform. Next, we incubated the sections for blocking in 1X PBS with 10% donor horse serum (DHS) for 1 hour at room temperature on a rocking platform. After blocking, we incubated the sections in PBS with 2.5% DHS and with primary antibodies for 48 hours at 4°C on a rocking platform. We then treated the slices with rabbit anti-phospho-S6 ribosomal protein (S235/6) antibody (1:100 dilution, Cell Signaling #2211) and wisteria floribunda lectin (WFA) biotinylated (1:1000 dilution, Vector Laboratories #B-1355-2).

After primary antibody incubation, we rinsed the sections twice with 0.4% PBS-T and then washed them in PBS-T three times for 15 minutes each. We incubated the sections with secondary antibodies in 450 µL of PBS with 2% DHS for 72 hours at 4°C on a rocking platform. We treated all sections with Alexa Fluor 488 goat anti-rabbit (1:200 dilution, Jackson ImmunoResearch Labs #111-605-144) and Cy3 streptavidin (1:5000 dilution, Vector Laboratories #SA-1300-1) secondary antibodies. We then rinsed the sections with 0.4% PBS-T and washed the sections with PBS-T three times for 15 minutes each. Last, we mounted the sections on Epredia Superfrost Microscope Slides with VectaShield Antifade Mounting Medium with DAPI (Vector Laboratories, #H-1200-10).

Confocal microscopy

We imaged all sections with a Zeiss LSM800 laser-scanning confocal microscope. We acquired z-stacks (1.5 μm interval, 0.7 digital zoom, and 512x512 pixel resolution) with a 40X oil objective lens. We acquired images of both hemispheres in prelimbic (PL), IL, and dentate gyrus (DG) in all rats. We took additional images if needed as we ran all immunohistochemistry in duplicate.

Image analysis

We analyzed fluorescence intensity with ImageJ/Fiji. We split the image into individual channels to quantify the intensities of pS6 and WFA separately. We processed each channel using the smooth function to remove pixel noise and then thresholded each channel, thereby maintaining consistent threshold values across rats and brain regions. We turned the threshold into a selection and split into individual regions of interest (ROIs). We measured the area and intensity individually per channel. We removed any ROI with an area under 10 μm^2 as this is smaller than any neuronal cell can be.

To assess the effects of the different interventions on mTOR and PNN activation we used general linear mixed effects models (LMEs) to detect group differences in mean intensity, 'Intensity ~ Sex + Age + Group'. We ran a separate model for each brain region. We used *coefTest()* for post-hoc analysis to determine the pairwise group differences.

Ethics statement

We carried out all experiments in accordance with NIH Guide for the Care and Use of Laboratory Animals (NIH Publications no. 80–23) revised in 1996 and approved by the Institutional Animal Care and Use Committee (IACUC) at Dartmouth College.

Results

LSD allows for a more stable and longer-lasting stimulation-induced brain state

Models built and tested on LFPs from before and 1 hour after stimulation (pre vs. post) outperformed permuted models in both groups ($p < 0.01$; **Fig. 2A**) with no effect of sex (**Extended Data Fig 2**). The post-stimulation brain activity of the LSD group was significantly easier to differentiate from pre-stim than that of the SAL group ($p < 0.01$; **Fig. 2A**). The change in brain activity detected by these models persisted across washout days in both groups compared to permuted models (Supplemental Data Table) but only the LSD group outperformed the overfit control models (**Fig. 2B**). Comparing LSD to SAL revealed that LSD significantly increased model performance ($\beta = 0.12$ [0.03 0.22], SE = 0.028, $t(6) = 3.16$, $p = 0.020$) with no effect of time or interaction between group and time (**Fig. 2B**). Post-hoc permutation tests showed the group difference occurred over the first 3 days ($p = 0.0099$, 0.030, and 0.020 respectively). The fact that the SAL data overlaps with the sham model performance (**Fig. 2B**; heavy black line) suggests that there are no persisting effects of stimulation alone. Although there is a decrease in velocity from pre to post stimulation, this difference does not allow a model built on velocity data to outperform chance in differentiating pre from post or pre from washout data (**Extended Data Figure 3**). Therefore, the performance of the pre vs. post models on both post and washout data can not be entirely explained by changes in velocity.

Not only was brain activity more changed in the LSD group for the first hour after stimulation, but the performance of the models on individual rats was less variable when given LSD (**Fig. 2C-D**). Using two-sample t-tests shows a decreased standard deviation in AUC for each rat across time (mean difference = -0.017 [-0.033 -0.0013], t(39) = -2.2, p = 0.034; **Fig. 2E**) and for each 5 minute time interval across rats (mean difference = -0.042 [-0.058 -0.027], t(22) = -5.6, p < 0.001; **Fig. 2F**). A representative top feature in the pre vs. post models for the LSD group was right mPFC to left NAcC alpha coherence. Plotting that feature through time as a z-score from pre-stimulation levels reveals the dynamics responsible for model performance and the difference in model performance between groups; it starts decreasing in both groups during stim, remains decreased for the hour after stim, and then returns to baseline immediately in the SAL group while taking a few days to return to baseline in the LSD group (**Fig. 2G**). Not only does LSD pretreatment allow for stimulation to push the brain further away from its baseline state (i.e., post-stimulation brain state is more differentiable from pre-stimulation brain state), but it also allows the brain to remain changed for days—stimulation alone acutely pushes the brain away from baseline, but the brain returns to baseline within 24 hours.

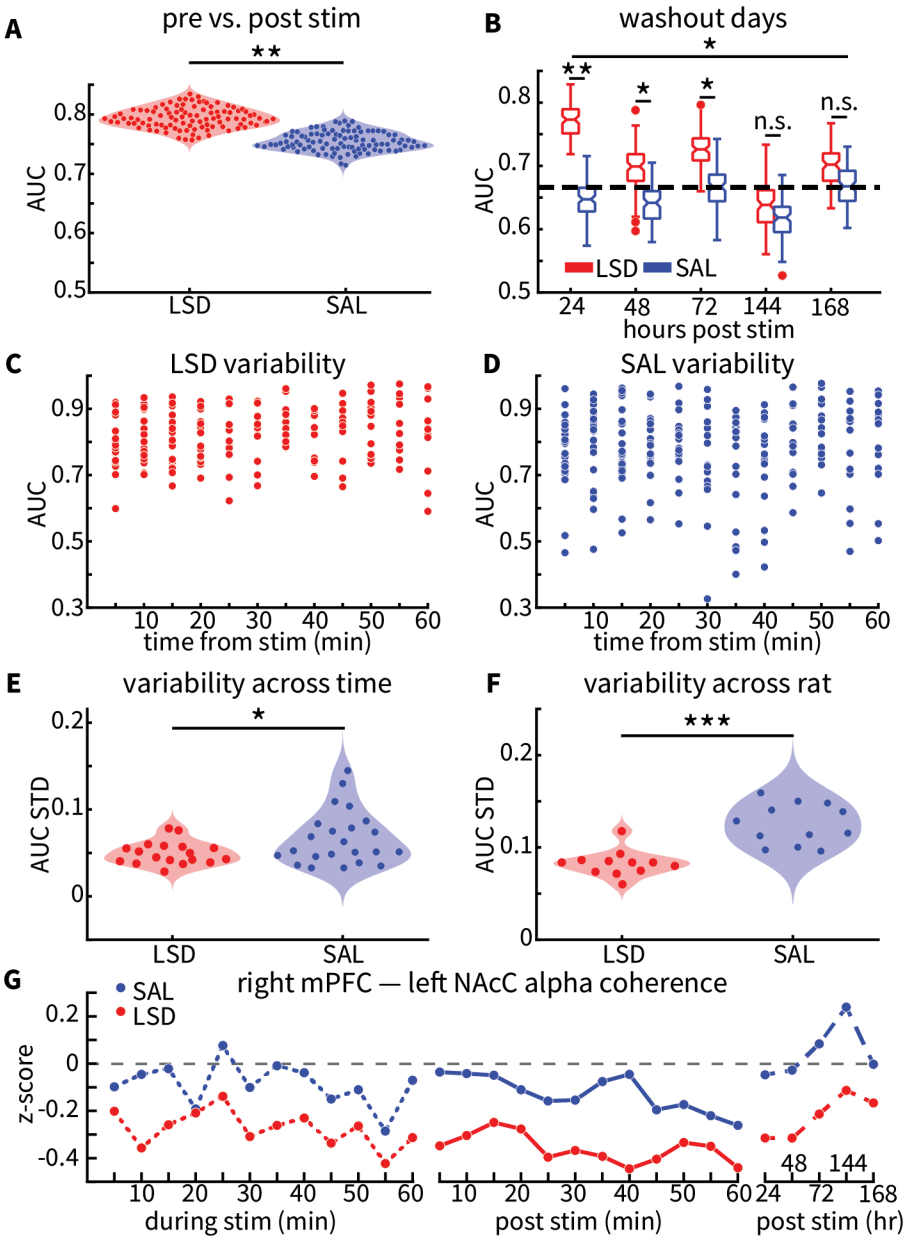

Fig. 2 LSD pretreatment allows for a large, longer-lasting, and stabler stimulation-induced brain state. **A.** Models built to differentiate pre-stimulation from post-stimulation neural data outperform chance (not shown) in either the LSD group (red) or saline group (SAL; blue) and there is a larger difference between pre and post data in the LSD group compared to the SAL group. **B.** LSD models outperform SAL models on washout days, for up to 3 days after stimulation. Heavy dashed black line indicates the estimated performance of overfit models from **Extended Data Figure 1**. **C-F.** The performance of the models in A on individual rats outperforms chance in LSD (**C**) and SAL (**D**) with less variability (standard deviation) in performance across time (**E**) and rats (**F**) in LSD vs. SAL for the first hour after stimulation. **G.** A representative feature, z-scored from baseline levels, shows shifts during stimulation in the LSD group that remain for 60 minutes and multiple days after stimulation. *** $p < 0.001$, ** $p < 0.01$, * $p < 0.05$, and n.s. = not significant.

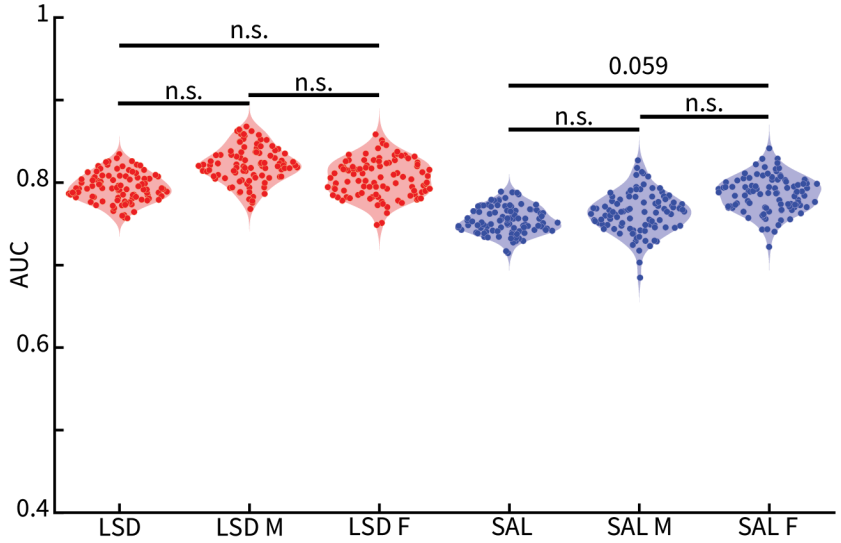

Extended Data Fig. 2 Pre vs. post models generalize across sex. Testing the pre vs. post models built on data from both sexes (**Fig. 1A)** on each sex separately revealed no difference in performance between sexes nor between each sex and the full test set.

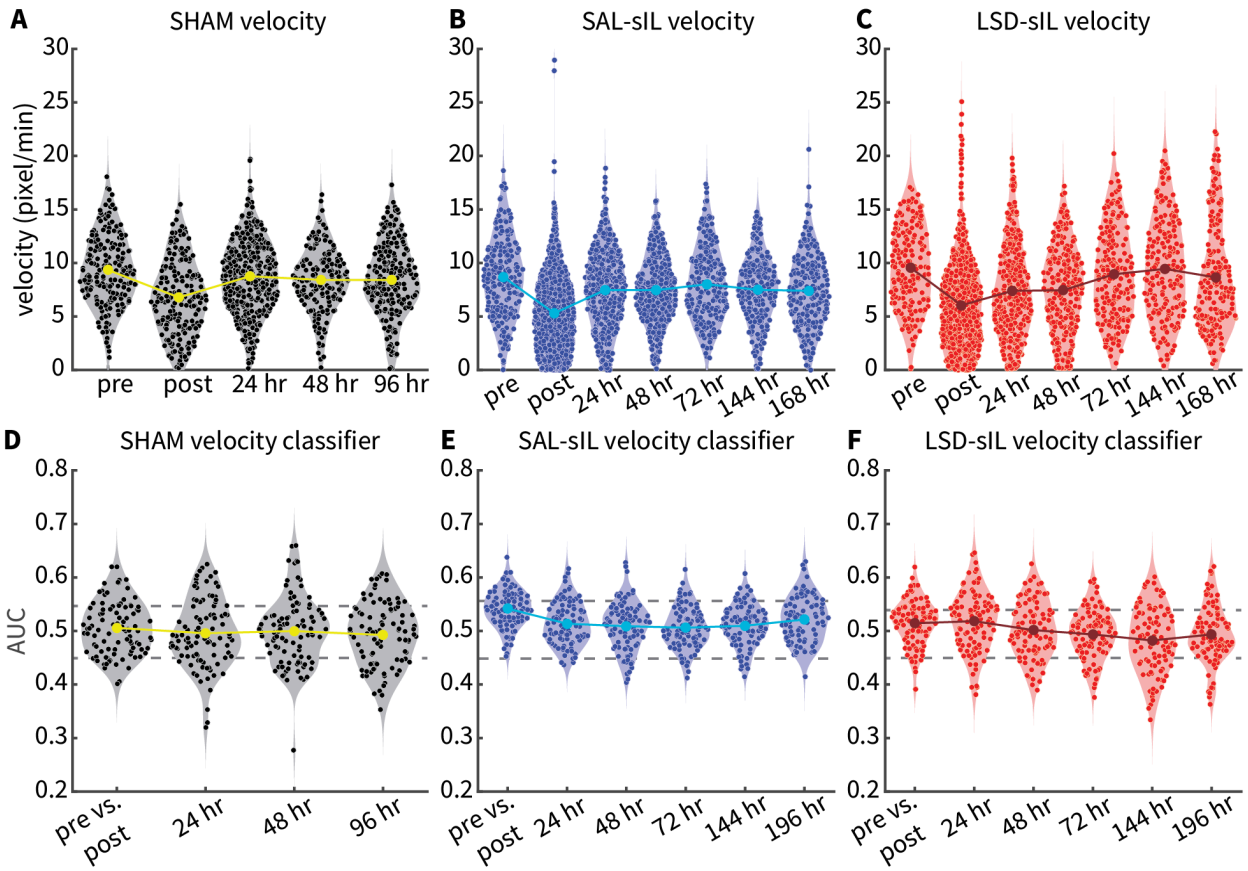

Extended Data Fig. 3 Velocity does not significantly contribute to model performance. **A-C.** Velocities (pixel/min) for each group across time corresponding to intervals used for LFP-based classifiers. Large circles and solid lines indicate average velocities. **D-F.** Performances of classifiers built from velocity data then tested across time. Large circles and solid lines indicate average AUCs and dashed grey lines indicate the mean±standard deviation of permuted classifier performance. No models outperform their corresponding permuted range.

LSD interacts with stimulation to produce a similar, but distinct brain state

We next compared the performance of single feature pre vs. post models tested on washout data between the LSD and SAL datasets to see if the same features were being persistently changed by stimulation regardless of whether rats had been given LSD or SAL. Using the distribution of permuted LSD single feature model performances, we set a 95% threshold revealing 14 LSD features. By sorting features by their performance in LSD data, we found that all LSD features outperforming chance performed better in the LSD group than the SAL group (**Fig. 3A**). As the SAL model did not outperform the overfit control on washout days (**Fig. 2B**) we then highlighted all the LSD features that outperformed the corresponding SAL feature—12 of the 14 LSD features that outperformed permuted models. Stimulation after LSD led to an increase in corticostriatal theta coherence alongside a decrease in alpha and beta power in NAcS and IL, increased IL-OFC high gamma coherence, increased right accumbal theta coherence, and increased OFC-NAcC alpha coherence (**Fig. 3B**) and these changes persisted into the washout days. Comparing the performance of these single feature models between the original pre vs. post data and the washout data from 24 hours after stimulation revealed that all ten models substantially increased in performance in the LSD data compared to the SAL data (**Fig. 3C**), indicating that these features were not only changed by stimulation for the first hour, but continued to change in the same direction over the next 24 hours–moving further from baseline. We then

directly compared the LSD and SAL pre vs. post models by cross-applying each which led to a significant decrease in performance in both cases (**Fig. 3D**). Furthermore, we built models to directly differentiate between LSD and SAL during stimulation and the first hour after stimulation, both of which significantly outperformed chance (**Fig. 3E**). That the cross-applied models do not fall to chance levels (~0.5) suggests that although LSD does significantly alter the effects of stimulation and the persistence of these effects, there is still some overlap between what stimulation does with or without LSD pretreatment.

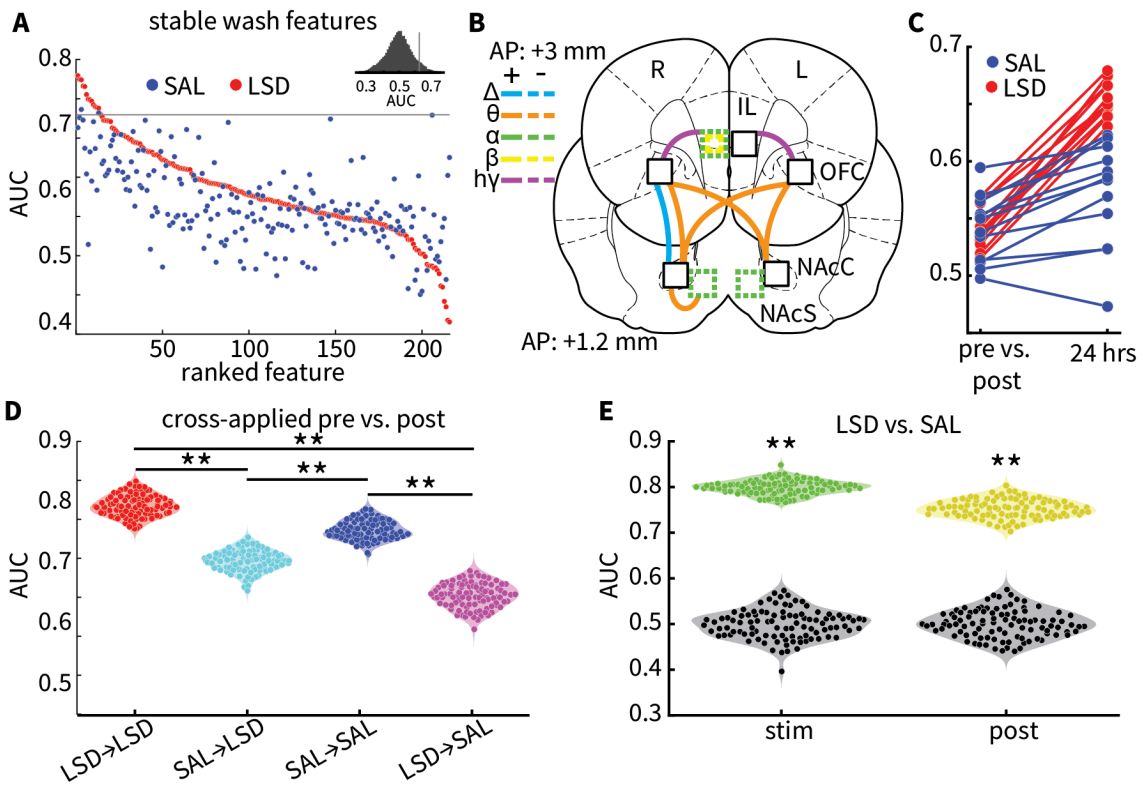

Fig. 3 LSD alters the effects of stimulation. **A.** Performance of single feature pre vs. post models on washout days, sorted by performance on LSD data. Red dots come from LSD data and blue from SAL. Horizontal grey line indicates 95% threshold of performance based on the distribution of LSD permuted single feature models (top inset). **B.** Map of the top 12 LSD features from **A** that outperform corresponding SAL models. Solid vs. dashed lines indicate if a given feature is increased or decreased post stimulation compared to pre stimulation. Lines connecting brain regions indicate coherence between those regions and colored outlines indicate power in that region. Color indicates frequency range. **C.** Comparison of the change in single feature model performance from the first hour after stimulation to 24 hours after for the top 12 features from **A** and **B**. LSD data in red and SAL in blue. **D.** Cross-applying models lowers performance in the first hour after stimulation compared to training and testing models within datasets. **E.** Models built to differentiate between LSD and SAL changes during stim (green) and during the hour after stimulation (yellow) outperform chance. ** $p < 0.01$.

Brain states induced by stimulation evolve over time

We were also able to build models to differentiate between pre-stim LFPs and LFPs during stimulation (pre vs. stim) that not only outperformed permuted models ($p < 0.01$; **Fig. 4A**), but also their corresponding pre vs. post models for both LSD ($p < 0.01$; **Fig. 4A**) and SAL groups ($p < 0.01$; **Fig. 4A**). However, applying these pre

vs. stim models to pre vs. post data significantly decreased performance ($p < 0.01$; **Fig. 4A**). Further, we compared the performance of the pre vs. post and pre vs. stim models on washout days and found that the pre vs. stim models performed worse than pre vs. post models in the LSD group ($\beta = -0.13$ [-0.22 -0.042], SE = 0.037, $t(6) = -3.60$, $p = 0.011$; **Fig. 4B**), but not the SAL group. A representative feature, left NAcS to right NAcS delta coherence, shows a robust decrease in both groups while stimulation is active that immediately returns to baseline levels when stimulation is turned off and throughout the washout days (**Fig. 4C**). Last, comparing the performance of single feature models from the LSD pre vs. stim models on pre vs. stim data and pre vs. wash data shows no significant correlation indicating that a feature that can detect when stimulation is on does not tend to also predict persistent changes and vice versa (**Fig. 4D**).

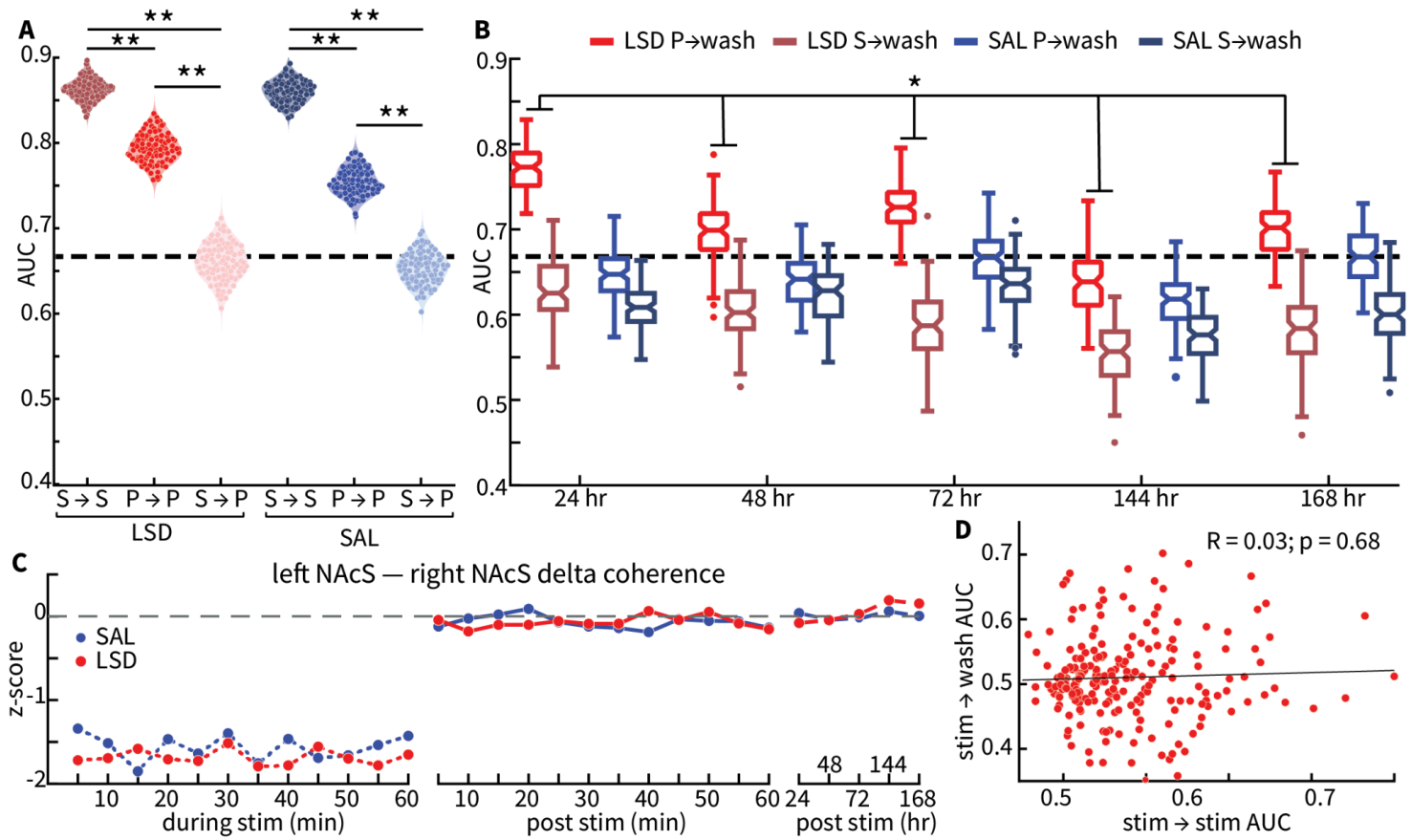

Fig 4 Brain states induced during stim do not persist, but states that emerge immediately after stim do. **A.** Building and training models within stim or post (S → S; P → P) outperforms a model trained on stim and tested on post (S → P). All models outperform chance. **B.** Models built on post data from the LSD group outperform models built on stim data from the LSD group. **C.** Representative features, z-scored from baseline levels, showing the dynamics of a feature changed by stimulation. Both groups show a decrease in left nucleus accumbens shell (NAcS) — right NAcS delta (Δ) coherence during stimulation, that immediately rebounds to baseline levels after stimulation and remains there through washout days. **D.** There is no correlation between single feature model performance (AUC) of models trained on pre vs. stim data and tested on pre vs. stim (x axis) or pre vs. wash (y axis) for LSD. ** $p < 0.01$, * $p < 0.05$, and n.s. = not significant. Heavy dashed black line in A and B indicates the estimated performance of overfit models from **Extended Data Figure 1**.

Cohort comparison

Since the two cohorts had different amounts of stimulation (1 hour for cohort 1 and 2 hours for cohort 2), we replicated all of the above analyses for each cohort on its own and saw the same overall effects: LSD elevated model performance for the first hour after stimulation (**Extended Data Fig. 4A-B**); the LSD model outperformed SAL for days after stimulation (**Extended Data Fig. 4E-F**); cross-applied models did worse than models trained and tested within the same group (**Extended Data Fig. 4C-D**); and LFPs during stimulation differed from those in the first hour after stimulation (**Extended Data Fig. 4G-H**). Despite an additional hour of stimulation, the pre vs. post models for the SAL group and LSD group from cohort 2 did not outperform their cohort 1 counterparts **Extended Data Fig. 4A-B**) nor did the performance of pre vs. post models applied to each of the first two washout days differ between cohorts (**Extended Data Fig. 4E-F**).

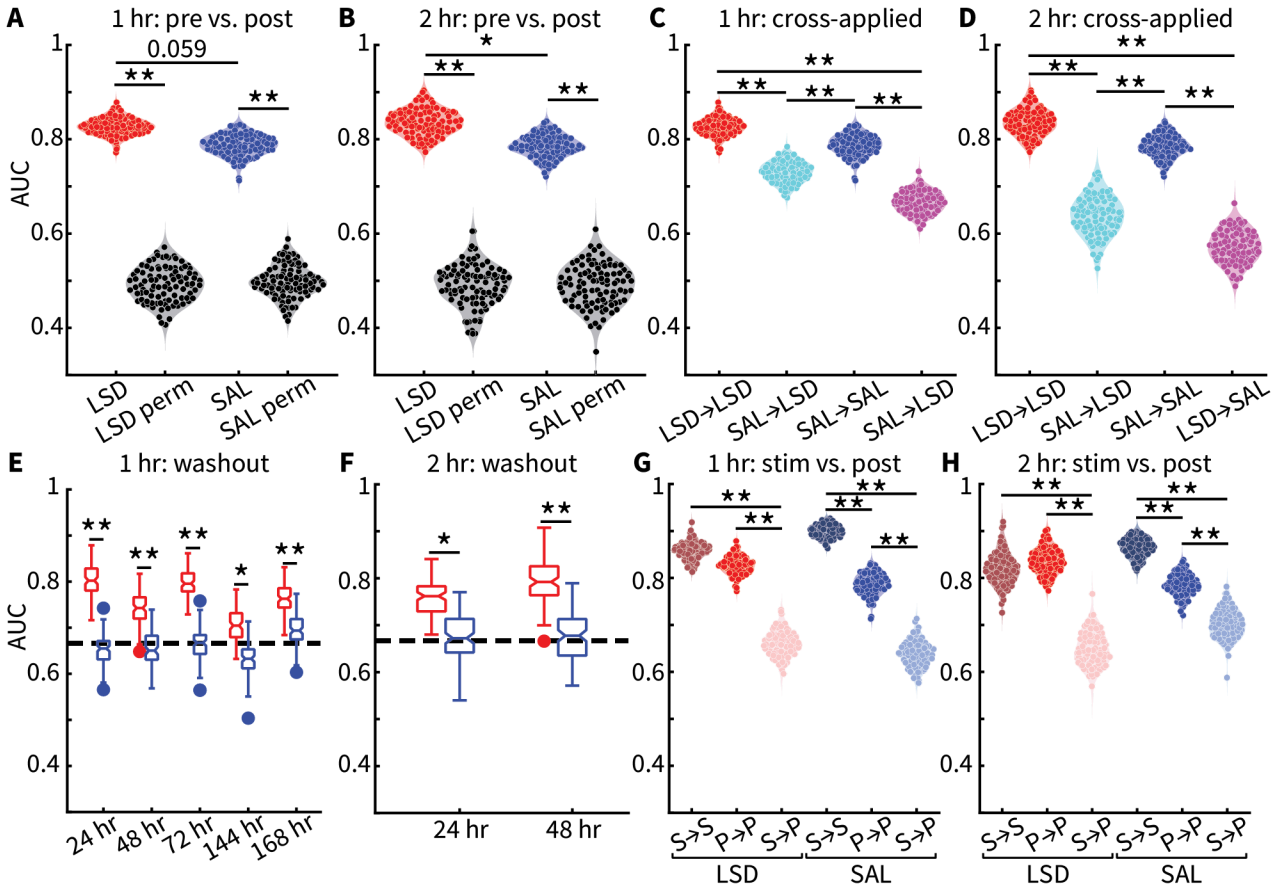

Extended Data Fig. 4 Both cohorts recapitulate the results of the combined cohorts. **A-B.** Pre vs. post models outperform chance (black distributions) and LSD outperforms saline (SAL) at a trend level for cohort 1 (1 hour stimulation; **A**) and significantly for cohort 2 (2 hours stimulation; **B**). **C-D.** Cross-applied models decrease performance in both cohorts. **E-F.** LSD pre vs. post models applied to washout days outperform SAL models and overfit control (heavy dashed line). **G-H.** Pre vs. stim models applied to pre vs. post data (S→P) results in a significant decrease in performance compared to either model tested on its own data (S→S or P→P) in both cohorts. ** $p < 0.01$, * $p < 0.05$

mTOR activation and PNN integrity

We found group differences in mTOR activation (pS6 intensity) in IL ($F(3,1156) = 4.319$, $p<0.005$; **Fig. 5A**) and mPFC ($F(3, 749) = 6.403$, $p < 0.001$; **Fig. 5B**), but not DG ($F(3,260) = 1.422$, $p = 0.24$; **Fig. 5C**). We found an effect of age in all regions, with increased mTOR activation in older rats: IL ($F(1,1156) = 9.026$, $p < 0.003$),

mPFC ($F(1,749) = 35.694$, $p < 0.001$), and DG ($F(1,260) = 19.011$, $p < 0.001$). We also found an effect of sex in IL ($F(1,749) = 9.935$, $p < 0.002$), with more activation in males. Post-hoc analysis revealed that the overall group difference in IL mTOR was driven by increased mTOR in LSD-sIL compared to LSD-sham ($p < 0.001$) and SAL-sham ($p = 0.026$); and increased mTOR in SAL-sIL compared to LSD-sham ($p = 0.011$). In the PL, the overall group difference in mTOR was driven by increased mTOR in LSD-sIL compared to LSD-sham ($p < 0.001$) and SAL-sham ($p = 0.011$); increased mTOR in SAL-sIL compared to LSD-sham ($p = 0.0018$); and increased mTOR in SAL-sham compared to LSD-sham ($p = 0.026$). Therefore, it appears that the increase in mTOR activation is largely driven by stimulation. However, if the upregulation of mTOR was entirely driven by stimulation, we would expect to see a similar increase in SAL-sIL compared to SAL-sham, which we do not observe. Therefore, despite not increasing mTOR beyond SAL-sIL, there may be an interaction between LSD pretreatment and IL stimulation.

We found group differences in PNN status (WFA intensity) in IL ($F(3,792) = 9.968$, $p < 0.001$; **Fig. 5D**) and DG ($F(3,1519) = 8.971$, $p < 0.001$; **Fig. 5F**), but not PL ($F(3,784) = 1.287$, $p = 0.28$; **Fig. 5E**). We found an effect of sex in all regions with more PNNs found in males: IL ($F(1,792) = 8.312$, $p = 0.004$), PL ($F(1,784) = 6.63$, $p = 0.01$), and DG ($F(1,1519) = 7.192$, $p = 0.007$). Last, we found an effect of age in PL ($F(1,784) = 13.598$, $p < 0.001$) and DG ($F(1,1519) = 5.461$, $p = 0.02$) with increased PNNs in older rats. Post-hoc analysis revealed that the overall group difference in IL PNNs was driven by increased PNNs in LSD-sIL compared to all other groups: LSD-sham ($p = 0.009$), SAL-sIL ($p < 0.001$), and SAL-sham ($p = 0.036$); and increased PNNs in LSD-sham compared to SAL-sIL ($p < 0.001$) and SAL-sham ($P < 0.001$). The overall group difference in DG PNNs was driven by increased PNNs in LSD-sIL compared to both LSD-sham ($p = 0.029$) and SAL-sham ($p < 0.001$); and increased PNNs in SAL-sIL compared to SAL-sham (< 0.001). Therefore, LSD alone is enough to increase PNN integrity in the IL and also interacts with stimulation to produce an even larger increase in PNN integrity.

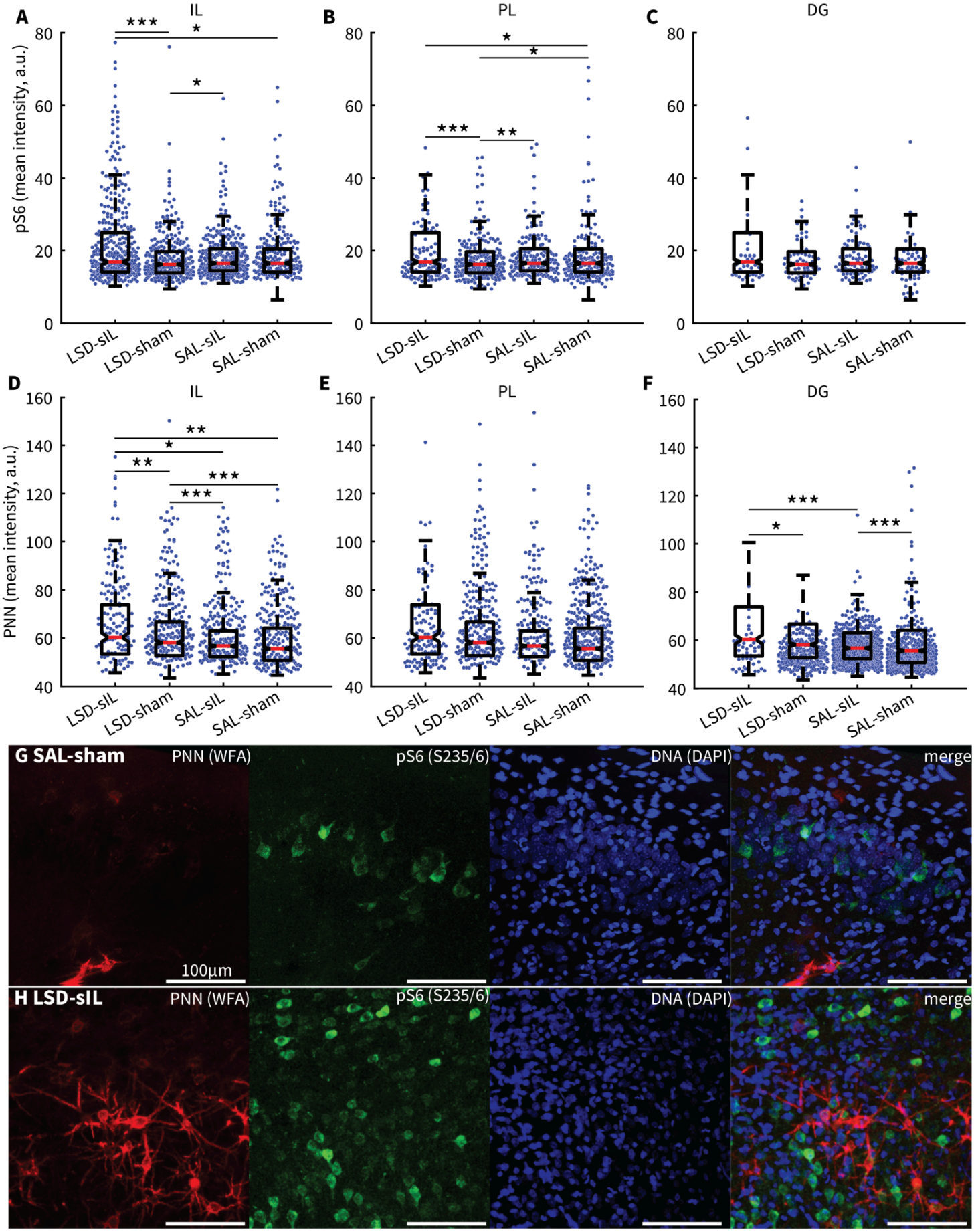
A
IL
B
PL
C
DG
pS6 (mean intensity, a.u.)
LSD-sIL
LSD-sham
SAL-sIL
SAL-sham
D
E
F
PNN (mean intensity, a.u.)
G SAL-sham
H LSD-sIL
PNN (WFA)
pS6 (S235/6)
DNA (DAPI)
merge
100µm

Fig. 5 LSD-sIL elevates mammalian target of rapamycin (mTOR) and perineuronal nets (PNN) in infralimbic cortex (IL). **A-C.** Phospho S6 staining intensity as a marker of mTOR activation across the 4 groups in 3 brain regions: IL (**A**), prelimbic cortex (PL; **B**), and dentate gyrus (DG; **C**). **D-F.** PNN staining across the 4 groups in the same 3 brain regions as **A-C**. **G-H.** Representative images of staining from a rat in the SAL-sham (**G**) and LSD-sIL (**H**) groups. Wisteria floribunda lectin (WFA) staining as a marker for PNN integrity in red, S235/6 staining for pS6 in green, DAPI for DNA in blue. Scale bar is 100 µm. *** $p < 0.001$, ** $p < 0.01$, * $p < 0.05$

Discussion

Here we show that LSD pretreatment allows for brain stimulation to push the brain further away from its baseline state, and that the brain remains altered for days longer than when stimulation is given after SAL. This means that psychedelics may allow for brain stimulation therapies like TMS to have longer lasting effects, reducing the high relapse rates currently limiting these non-invasive stimulation approaches. We also show that the shifts in brain activity during stimulation differ from the shifts in brain activity that evolve once stimulation has ended; importantly, it is the post-stimulation brain state that is maintained for days after stimulation and would support any therapeutic effect, not the brain state during stimulation. This means that using brain activity states recorded during stimulation may not reflect the stable long term changes that carry therapeutic effects through time and thus serve as poor biomarkers to tune stimulation parameters.

LSD allows for larger and longer-lasting effects of brain stimulation

By stimulating the IL in the group given LSD 24 hours prior, we are able to produce stable, long-lasting changes in brain activity that are distinguishable from those produced in the group given SAL. The LSD pre vs. post model had higher performance and this performance was much more stable through time for both the 1 hour immediately after stimulation and the subsequent days. In addition, although there is overlap in the effects of stimulation regardless of pretreatment, we also show that LSD allows for stimulation to produce new effects on brain activity. These results suggest that psychedelics like LSD could be used as an adjuvant therapy alongside neuromodulation to promote long-lasting changes in brain activity and thus mood/mindset. Although we did include a model that captures the change in LFPs across time that are unrelated to any intervention (sham model), we do not have washout LFPs from rats only given LSD. Therefore, we can not be certain that our persistent changes in brain activity in rats given LSD before stimulation are not at least in part due to residual effects of LSD alone nor the stacked effect of two stimulation sessions. However, in our previous work we showed that despite LSD producing robust effects on LFPs acutely, these effects are largely gone by 24 hours and models are no longer able to distinguish between a rat given SAL or LSD the day prior [25]. Given that SAL+sIL does not produce persistent changes in brain activity, it seems unlikely that the SAL+sIL session would be interacting with the LSD+sIL session 1 week later to produce persisting effects after LSD+sIL. However, it could be the case that the first stimulation session is producing latent changes in the brain or persisting effects that are not captured by LFP power and coherence. There are three possible solutions to this worth considering for future work, although each solution has its own limitations: 1. Counterbalancing the experimental design such that half of the rats receive LSD+sIL first and half receive SAL+sIL first; 2. Using entirely different groups of rats that only receive one intervention pair; and 3. Maintaining the order and increasing the duration between interventions.

We found at least a 3-fold increase in the duration of stimulation induced brain state when pretreated with LSD (i.e., SAL+stim alters brian activity for at least 1 hour on the same day as stimulation while LSD+stim alters brain activity for at least 3 days after stimulation); if this translated to humans, we could see prolonged therapeutic effects for additional months to years after a course of non-invasive stimulation. Granted, there are many differences between our 1-hour stimulation session in wild-type rats and multiple hours of stimulation across many sessions in patients, so the translation of our results to clinical populations is likely not straightforward. For example, a longer treatment course after stimulation may lead to even more persistent brain changes or given the state dependency of stimulation's effects [33–36], stimulation in a patient may produce more or less effects than in a healthy brain.

Others have already demonstrated the potential for neuroplastic modulators (i.e., the NDMA partial agonist D-cycloserine) to enhance the effects of TMS [23,24]. Other serotonergic psychedelics, like 2,5-dimethoxy-4-iodoamphetamine (DOI) has also been shown to modulate neuroplastic processes with pretreatment allowing for enhanced induction of long-term potentiation (LTP) [37,38] and concurrent administration reversing the polarity of plasticity induced in the claustrum to anterior cingulate cortex neurons from long-term depression to LTP [39]. Interestingly, although psychedelics have not yet been paired with therapeutic stimulation in humans, both ketamine and psilocybin have been paired acutely with TMS pulses and neither showed any impact on the complexity of evoked responses [40,41]. It could be the case that these concurrent protocols do not allow enough time for neuroplastic processes to be engaged.

We hypothesize that psychedelic pretreatment produces a malleable state in which dendritic spines are more likely to be in an 'immature' state and neurons are primed for neuroplastic processes. By applying brain stimulation in this state, we are able to produce more robust changes in brain circuits than stimulation is able to produce on its own[42]. Likely the timing between psychedelics and stimulation is a critical factor in maximizing their interaction. For example, psychedelics alter the proportion of mature and immature spines within 24 hours [9,38], but at longer timepoints (e.g., 34 days and 12 weeks) this shift disappears [43,44] — suggesting a resettling of neural circuits and highlighting a timeframe in which stimulation may have the best chance to guide the reshaping of neural circuits.

It is worth noting that the neural features that remain altered for days after stimulation are predominately measures of coherence. This suggests that stimulation after LSD is able to produce long-lasting changes in the connectivity between brain regions, in this case increasing the connectivity of the OFC and NAc. Interestingly, the stimulation target was the IL and not the OFC or NAc. Future work should test stimulation targeting a variety of nodes in the frontostriatal network with high frequency stimulation after LSD to determine if they all produce the same increased persistence of stimulation-induced changes with convergent increases in frontal-striatal theta coherence. It may also be the case that LSD pretreatment allows for persistent effects of stimulation, but the features changed depend on the stimulation target; alternatively, the persistence itself may also depend on targeting. Likewise, other stimulation protocols (e.g., low frequency stimulation or stimulating for multiple hours/days) may also alter the interaction of stimulation with psychedelic pretreatment. Last, LSD is not the only psychedelic drug with neuroplastic effects; other shorter-acting psychedelics like psilocybin and N,N-dimethyltryptamine (DMT) also produce neuroplastic effects and may be more palatable for clinical use. Thus, there are multiple important avenues of future research to better understand the full potential of psychedelic-assisted brain stimulation.

Brain states induced by stimulation evolve over time

By building and testing our models at different periods in our experiment, we have shown that the brain state that occurs during stimulation is not the same as the brain state that arises in the hour or days after stimulation. Further, the brain state produced in the hour after stimulation is more indicative of what will remain changed days later compared to the brain state produced during stimulation. At the level of individual features these changes are often subtle and exhibit interesting temporal dynamics. Of note, the features that are most changed during stimulation are often not the same features that are changed immediately after stimulation or days later. Instead, we find a handful of features that exhibit either marginal or no changes during stimulation, that then change when stimulation is turned off, and then remain changed for days. We also find some features that are changed in the first hour after stimulation, but don't remain changed in subsequent days. Clinically, it has been shown that the effects of deep brain stimulation (DBS) on brain activity evolve through time with the LFP features most predictive of clinical outcome first showing an acute decrease with stimulation that over many days increases relative to baseline and it is this increase that correlates with clinical benefit [45]. Similarly, in repetitive TMS for cocaine use disorder, the ability for TMS to create a lasting shift in brain state dynamics (i.e., increasing the duration of a specific brain state) correlated with a sustained decrease in cravings [46].

This means that for both acute and chronic brain stimulation there are likely complex dynamics of brain state change with the changes elicited immediately during stimulation not necessarily reflecting the changes that will persist beyond active stimulation or develop with chronic stimulation and lead to a therapeutic response. Therefore, even with empirical, brain activity-based biomarkers relevant to psychiatric disorders, optimizing stimulation parameters may not be able to rely on high-throughput screening over dozens or hundred of parameters in a single session. Instead, effective optimization may take multiple sessions over days or weeks.

Clinical outcomes and brain state stability

The theoretical framework of this work is that successful psychiatric treatment is built upon long-lasting shifts in brain state and that relapse occurs when the brain relaxes back to its pre-treatment state; therefore, by prolonging the effects of brain stimulation with psychedelics we demonstrate a novel approach to reduce relapse rates. Besides the above evidence that DBS induced changes in brain activity correlate with clinical benefit for depression [45], there is also a rich literature from Parkinson's disease suggesting that beta oscillations can serve as a similar biomarker of successful treatment and relapse of motor symptoms [47]. There is also evidence that depression relapse correlates with decreased network resilience/stability [48,49] while never-depressed controls and sustained remission correlates with increased network stability [49]. In remitted depression, residual symptoms tend to correlate with maintained disruptions in connectivity [50]. However, it is worth noting that there is also evidence that depression relapse leads to a network structure more similar to healthy controls than remission [51]. This suggests that the brain states underlying 'healthy', 'remission', and 'relapse' may have a more complex relationship than remission merely consisting of getting the brain back to its healthy state; instead, relapse is associated with the inability to establish a stable network structure. Our work suggests that psychedelics can help brain stimulation produce such stable changes in brain activity.

mTOR is upregulated by LSD and stimulation

Stimulation led to more mTOR activation than the corresponding control groups and LSD pretreatment led to the highest level of mTOR activation. Although our LSD-sIL groups have more mTOR activation than LSD-sham or SAL-sham in IL and PL, this is likely driven by stimulation as the LSD-sIL does not have more mTOR activation than SAL-sIL. However, if the upregulation of mTOR was entirely driven by stimulation, we would expect to see a similar increase in SAL-sIL compared to SAL-sham, which we do not see. So although others find that mTOR upregulation by psychedelics does not last 24 hours [52] and stimulating sooner may create a larger interaction effect, we provide evidence of an interaction between LSD given 24 hours before and brain stimulation.

The evidence of classic psychedelics like LSD altering mTOR activation is growing [6–10]) and there is a plethora of evidence for the role of mTOR in the neuroplastic and antidepressant effects of ketamine [53–61] (for review [62–64]) and other antidepressants [53,65–69]. However, not all antidepressants seem to act through mTOR [68]. One of the leading theories for how psychedelics are able to produce long-lasting clinical benefits is that they modulate neuroplasticity, allowing for structural and functional changes in the neural circuits underpinning disorders. Although there is a strong theoretical foundation for this theory and there is growing preclinical evidence for the alteration of dendritic spines, there is evidence that psychedelics may enhance LTP mechanisms *in vitro* [37] and alter the effects of brain stimulation *in vivo* [25]. Prior work has demonstrated that one hour of IL stimulation can alter depression-like behaviors in rodents, and also upregulate AKT and CREB phosphorylation, all of which were blocked by temsirolimus (an mTOR antagonist) [11]. However, no change in mTOR phosphorylation was found, which was attributed to looking too long after stimulation (3-4 hours). Others have found that the upregulation of mTOR from ketamine is present at 1 hour post administration, but not 6 hours [53]. Another study saw upregulation of mTOR after chronic ventromedial PFC stimulation (1 hour every day for 18 days) that was measurable at ~1.5 hours after the last stimulation session as increased brain-derived neurotrophic factor (BDNF), AKT, mTOR, and CREB activation in the hippocampus alongside amelioration of behavioral and synaptic deficits induced by chronic unpredictable stress [13]. In a study targeting lateral habenula with stimulation for 4 days of 1 hour sessions, hippocampal mTOR was upregulated 30 minutes after the last stimulation session [70].

Although mTOR is at the 'crossroads' of plasticity, learning and memory, and is implicated in neuropsychiatric conditions [71], mTOR is but one node in a complex network of overlapping signalling pathways [72] with many up- and downstream signaling components. A key upstream regulator of mTOR is activation of tropomyosin receptor kinase B (trkB) by BDNF [73,74]. Of note, both brain stimulation and psychedelics have been shown to influence BDNF/trkB signalling. Stimulation not only increases BDNF [11,75–79], but that increase also correlates with symptom reduction[80,81] and is related to neuroplastic processes [82]. While some of these studies saw increases in BDNF in healthy controls [75,76] others only saw an effect in disease models and not controls [11,78,79]. There is also evidence that the effects of psychedelics on mTOR is mediated through BDNF/trkB [8,9] and may potentially be binding directly to trkB to enhance binding efficiency of BDNF[52].

It is not surprising that we saw an effect of age on mTOR activation as mTOR is known to be a key modulator of aging [83] and mTOR activation tends to be upregulated as animals age [84–87]. Likewise, our finding of increased mTOR activation in males is also seen in the literature; although there does appear to be more

variation in the effects of sex on mTOR activation depending on cell type/organ system and hormonal phase [88,89].

LSD and stimulation interact to increase PNN integrity

We found that although LSD alone is enough to increase PNN staining intensity in the IL, LSD pretreatment interacts with IL stimulation to produce an even larger increase in PNN staining. PNNs play a key role in regulating synaptic transmission [90,91] and plasticity such that their accumulation around neurons signals the closure of critical periods [92,93]. PNNs have been associated with early life adversity [94,95], memory [96,97], neuroinflammation [98], and thus may offer a promising avenue for neuropsychiatric treatments [99,100]. Although there is little known about the effects of psychedelics on PNNs, ketamine has been shown to alter PNNs; in a chronic administration paradigm involving 10 ketamine injections over 12 days, researchers have found both decreases [101] and increases [102] in mPFC PNNs in Sprague-Dawley rats. The increased PNNs did show morphological differences from controls with small and less circular PNNs, however it remains unclear what effect these differences have on neuronal function and plasticity [102]. Last, 3 ketamine injections in a stroke model ameliorated both the stroke-induced inflammation and behaviors while decreasing PNNs in unspecified 'cortex' in C57BL/J6 mice [103]. We found that a single dose of LSD increased IL PNNs compared to SAL and that although stimulation further increased PNNs in the LSD group, there was no effect of stimulation in the SAL group. Although LSD-stim increased PNNS in DG compared to LSD-sham and SAL-sIL, the effect was no more than in SAL-sham, so it may be the case that the hippocampal effects are more dependent on stimulation than LSD. A more thorough examination of the timeline of PNN phenotypes under LSD treatment would help elucidate whether serotonergic psychedelics first disrupt PNNs, allowing for plasticity, and then facilitate PNN reassociation, thereby locking in the induced synaptic changes. Further, it will be important to determine if psychedelics differentially alter the proportion of specific cell types associated with PNNs (e.g., PV+ vs. PV- interneurons).

With respect to our finding of increased PNNs in males and in older rats, the literature is complex. Depending on the exact age and brain region some have found slight decreases in cortical PNNs in very old mice (P590-734)[104], while others found increased PNNs in PFC, hippocampus, and somatosensory cortex of mice and rats between 1 to 2 years old[105–107], and still others see an increase in PNNs number during early development which then plateau in adolescence and PNN intensity continues to rise into adolescence[108]. Of note, there is also evidence that although WFA staining can identify PNNs, there are subtle changes in the molecular composition of PNNs through time which are missed with WFA staining, but can play a role in PNN function[109,110]. Last, there are hormonal effects on PNNs during puberty[111] and throughout the estrous cycle[112,113]; however, these differences are brain region-dependent[114] and overall sex differences in adulthood are mixed[115,116]. Given the role of PNNs in neuroplasticity, it is likely that both age and sex can modulate their distribution and function, but this study was not adequately powered to assess such factors rigorously, especially in the context of additional interventions (stimulation and pharmacology) which may also interact with age and sex.

Conclusion

We have confirmed that LSD given 24 hours before brain stimulation not only allows stimulation to induce larger changes in brain activity, but that these changes persist for days as compared to hours when

stimulation follows SAL. Further we have shown that LSD and brain stimulation may be interacting through an upregulation of mTOR signaling and increased PNNs. Combined with the known effects of psychedelics on neuroplasticity, these findings suggest that psychedelics produce a state of enhanced neuroplasticity that can then be acted upon by targeted brain stimulation to create lasting changes in brain activity of a larger neural circuit. Being able to direct neuroplasticity with focal brain stimulation to produce long lasting changes in neural circuits could allow for the persistent shifts in mindset and behavior sought for in neuropsychiatric treatments.

1. Raison CL, Sanacora G, Woolley J, Heinzerling K, Dunlop BW, Brown RT, et al. Single-Dose Psilocybin Treatment for Major Depressive Disorder: A Randomized Clinical Trial. JAMA. 2023;330: 843–853.

2. Rosenblat JD, Meshkat S, Doyle Z, Kaczmarek E, Brudner RM, Kratiuk K, et al. Psilocybin-assisted psychotherapy for treatment resistant depression: A randomized clinical trial evaluating repeated doses of psilocybin. Med. 2024;5: 190–200.e5.

3. Krebs TS, Johansen P-Ø. Lysergic acid diethylamide (LSD) for alcoholism: meta-analysis of randomized controlled trials. J Psychopharmacol. 2012;26: 994–1002.

4. Bogenschutz MP, Ross S, Bhatt S, Baron T, Forcehimes AA, Laska E, et al. Percentage of Heavy Drinking Days Following Psilocybin-Assisted Psychotherapy vs Placebo in the Treatment of Adult Patients With Alcohol Use Disorder: A Randomized Clinical Trial. JAMA Psychiatry. 2022;79: 953–962.

5. Brett B, Bynum C. MDMA-Assisted Psychotherapy for PTSD: A Systematic Review of Randomized Control Trials. J Psychoactive Drugs. 2025; 1–13.

6. Wang Z, Robbins B, Zhuang R, Sandini T, van Bruggen R, Li X-M, et al. Early psilocybin intervention alleviates behavioral despair and cognitive impairment in stressed Wistar rats. Prog Neuropsychopharmacol Biol Psychiatry. 2025;136: 111243.

7. Du Y, Li Y, Zhao X, Yao Y, Wang B, Zhang L, et al. Psilocybin facilitates fear extinction in mice by promoting hippocampal neuroplasticity. Chin Med J (Engl). 2023;136: 2983–2992.

8. Ly C, Greb AC, Vargas MV, Duim WC, Grodzki ACG, Lein PJ, et al. Transient Stimulation with Psychoplastogens Is Sufficient to Initiate Neuronal Growth. ACS Pharmacol Transl Sci. 2021;4: 452–460.

9. Ly C, Greb AC, Cameron LP, Wong JM, Barragan EV, Wilson PC, et al. Psychedelics Promote Structural and Functional Neural Plasticity. Cell Rep. 2018;23: 3170–3182.

10. De Gregorio D, Popic J, Enns JP, Inserra A, Skalecka A, Markopoulos A, et al. Lysergic acid diethylamide (LSD) promotes social behavior through mTORC1 in the excitatory neurotransmission. Proc Natl Acad Sci U S A. 2021;118. doi:10.1073/pnas.2020705118

11. Jiménez-Sánchez L, Linge R, Campa L, Valdizán EM, Pazos Á, Díaz Á, et al. Behavioral, neurochemical and molecular changes after acute deep brain stimulation of the infralimbic prefrontal cortex. Neuropharmacology. 2016;108: 91–102.

12. Chang H, Wang Y, Hui L, Diao Y, Ma P, Li X, et al. iTRAQ proteomic analysis of the anterior insula in morphine-induced conditioned place preference rats with high-frequency deep brain stimulation intervention. Addict Biol. 2025;30: e70014.

13. Sun Z, Jia L, Shi D, He Y, Ren Y, Yang J, et al. Deep brain stimulation improved depressive-like behaviors and hippocampal synapse deficits by activating the BDNF/mTOR signaling pathway. Behav Brain Res.

2022;419: 113709.

14. Fink M. What was learned: studies by the consortium for research in ECT (CORE) 1997-2011. Acta Psychiatr Scand. 2014;129: 417–426.

15. Sackeim HA, Haskett RF, Mulsant BH, Thase ME, Mann JJ, Pettinati HM, et al. Continuation pharmacotherapy in the prevention of relapse following electroconvulsive therapy: a randomized controlled trial. JAMA. 2001;285: 1299–1307.

16. Cohen RB, Boggio PS, Fregni F. Risk factors for relapse after remission with repetitive transcranial magnetic stimulation for the treatment of depression. Depress Anxiety. 2009;26: 682–688.

17. Senova S, Cotovio G, Pascual-Leone A, Oliveira-Maia AJ. Durability of antidepressant response to repetitive transcranial magnetic stimulation: Systematic review and meta-analysis. Brain Stimul. 2019;12: 119–128.

18. Diefenbach GJ, Bragdon LB, Zertuche L, Hyatt CJ, Hallion LS, Tolin DF, et al. Repetitive transcranial magnetic stimulation for generalised anxiety disorder: a pilot randomised, double-blind, sham-controlled trial. Br J Psychiatry. 2016;209: 222–228.

19. Watts BV, Landon B, Groft A, Young-Xu Y. A sham controlled study of repetitive transcranial magnetic stimulation for posttraumatic stress disorder. Brain Stimul. 2012;5: 38–43.

20. Boggio PS, Rocha M, Oliveira MO, Fecteau S, Cohen RB, Campanhã C, et al. Noninvasive brain stimulation with high-frequency and low-intensity repetitive transcranial magnetic stimulation treatment for posttraumatic stress disorder. J Clin Psychiatry. 2010;71: 992–999.

21. Cole EJ, Phillips AL, Bentzley BS, Stimpson KH, Nejad R, Barmak F, et al. Stanford Neuromodulation Therapy (SNT): A Double-Blind Randomized Controlled Trial. Am J Psychiatry. 2022;179: 132–141.

22. Geoly AD, Stimpson KH, Espil FM, Bentzley BS, Williams NR. Durability of clinical benefit with Stanford Neuromodulation Therapy (SNT) in treatment-resistant depression. Brain Stimul. 2025;18: 875–881.

23. Cole J, Selby B, Ismail Z, McGirr A. D-cycloserine normalizes long-term motor plasticity after transcranial magnetic intermittent theta-burst stimulation in major depressive disorder. Clin Neurophysiol. 2021;132: 1770–1776.

24. Cole J, Sohn MN, Harris AD, Bray SL, Patten SB, McGirr A. Efficacy of Adjunctive D-Cycloserine to Intermittent Theta-Burst Stimulation for Major Depressive Disorder: A Randomized Clinical Trial. JAMA Psychiatry. 2022;79: 1153–1161.

25. Dwiel L, Henricks A, Bragg E, Nicol J, Gui J, Doucette W. Lysergic Acid Diethylamide Alters the Effects of Brain Stimulation in Rodents. Psychedelic Med (New Rochelle). 2023;1: 43–53.

26. Sorg BA, Berretta S, Blacktop JM, Fawcett JW, Kitagawa H, Kwok JCF, et al. Casting a Wide Net: Role of Perineuronal Nets in Neural Plasticity. J Neurosci. 2016;36: 11459–11468.

27. Frischknecht R, Heine M, Perrais D, Seidenbecher CI, Choquet D, Gundelfinger ED. Brain extracellular matrix affects AMPA receptor lateral mobility and short-term synaptic plasticity. Nat Neurosci. 2009;12: 897–904.

28. Quansah Amissah R, Albeely AM, Bragg EM, Perreault ML, Doucette WT, Khokhar JY. A Simple, Lightweight, and Low-Cost Customizable Multielectrode Array for Local Field Potential Recordings.

eNeuro. 2023;10. doi:10.1523/ENEURO.0212-23.2023

29. Huybers P. Multi-taper coherence with bias correction. MATLAB Central File Exchange; 2016. Available: https://www.mathworks.com/matlabcentral/fileexchange/22551-multi-taper-coherence-method-with-bias-correction

30. Nolte G, Bai O, Wheaton L, Mari Z, Vorbach S, Hallett M. Identifying true brain interaction from EEG data using the imaginary part of coherency. Clin Neurophysiol. 2004;115: 2292–2307.

31. Phipson B, Smyth GK. Permutation P-values should never be zero: calculating exact P-values when permutations are randomly drawn. Stat Appl Genet Mol Biol. 2010;9: Article39.

32. Mathis A, Mamidanna P, Cury KM, Abe T, Murthy VN, Mathis MW, et al. DeepLabCut: markerless pose estimation of user-defined body parts with deep learning. Nat Neurosci. 2018;21: 1281–1289.

33. Deco G, Cruzat J, Cabral J, Tagliazucchi E, Laufs H, Logothetis NK, et al. Awakening: Predicting external stimulation to force transitions between different brain states. Proc Natl Acad Sci U S A. 2019;116: 18088–18097.

34. Wang S, Wen H, Qiu S, Xie P, Qiu J, He H. Driving brain state transitions in major depressive disorder through external stimulation. Hum Brain Mapp. 2022;43: 5326–5339.

35. Silvanto J, Cattaneo Z. Nonlinear interaction between stimulation intensity and initial brain state: Evidence for the facilitatory/suppressive range model of online TMS effects. Neurosci Lett. 2021;742: 135538.

36. Bradley C, Nydam AS, Dux PE, Mattingley JB. State-dependent effects of neural stimulation on brain function and cognition. Nat Rev Neurosci. 2022;23: 459–475.

37. Zahid Z, Sultan ZW, Krause BM, Wenthur CJ, Pearce RA, Banks MI. Divergent Effects of Ketamine and the Serotoninergic Psychedelic 2,5-Dimethoxy-4-Iodoamphetamine on Hippocampal Plasticity and Metaplasticity. Psychedelic Med (New Rochelle). 2024;2: 166–177.

38. de la Fuente Revenga M, Zhu B, Guevara CA, Naler LB, Saunders JM, Zhou Z, et al. Prolonged epigenomic and synaptic plasticity alterations following single exposure to a psychedelic in mice. Cell Rep. 2021;37: 109836.

39. Anderson TL, Asadipooya A, Ortinski PI. Psychedelics Reverse the Polarity of Long-Term Synaptic Plasticity in Cortical-Projecting Claustrum Neurons. eNeuro. 2025;12. doi:10.1523/ENEURO.0047-25.2025

40. Ort A, Smallridge JW, Sarasso S, Casarotto S, von Rotz R, Casanova A, et al. TMS-EEG and resting-state EEG applied to altered states of consciousness: oscillations, complexity, and phenomenology. iScience. 2023;26: 106589.

41. Farnes N, Juel BE, Nilsen AS, Romundstad LG, Storm JF. Increased signal diversity/complexity of spontaneous EEG, but not evoked EEG responses, in ketamine-induced psychedelic state in humans. PLoS One. 2020;15: e0242056.

42. Jiang Q, Shao L-X, Yao S, Savalia NK, Gilbert AD, Davoudian PA, et al. Psilocybin triggers an activity-dependent rewiring of large-scale cortical networks. Cell. 2025. doi:10.1016/j.cell.2025.11.009

43. Kramer HM, Hibicke M, Middleton J, Jaster AM, Kristensen JL, Nichols CD. Psychedelics produce enduring

behavioral effects and functional plasticity through mechanisms independent of structural plasticity. Neuropsychopharmacology. 2025. doi:10.1038/s41386-025-02272-3

44. Shao L-X, Liao C, Gregg I, Davoudian PA, Savalia NK, Delagarza K, et al. Psilocybin induces rapid and persistent growth of dendritic spines in frontal cortex in vivo. Neuron. 2021;109: 2535–2544.e4.

45. Alagapan S, Choi KS, Heisig S, Riva-Posse P, Crowell A, Tiruvadi V, et al. Cingulate dynamics track depression recovery with deep brain stimulation. Nature. 2023;622: 130–138.

46. Le C, Hou T, Zhu Y, Zhang Y, Ling J, Li Z, et al. Dynamic brain network reconfiguration following rTMS in males with cocaine use disorder. Front Hum Neurosci. 2025;19: 1603888.

47. Radcliffe EM, Baumgartner AJ, Kern DS, Al Borno M, Ojemann S, Kramer DR, et al. Oscillatory beta dynamics inform biomarker-driven treatment optimization for Parkinson's disease. J Neurophysiol. 2023;129: 1492–1504.

48. Homiack D, Boyd B, Zhang A, Begnoche JP, Butters M, Andreescu C, et al. Altered Dynamic Network Stability in Remitted Late Life Depression Associated with Depression Recurrence. Biol Psychiatry Cogn Neurosci Neuroimaging. 2025. doi:10.1016/j.bpsc.2025.08.013

49. Alonso S, Tyborowska A, Ikani N, Mocking RJT, Figueroa CA, Schene AH, et al. Depression recurrence is accompanied by longer periods in default mode and more frequent attentional and reward processing dynamic brain-states during resting-state activity. Hum Brain Mapp. 2023;44: 5770–5783.

50. Peters AT, Burkhouse K, Feldhaus CC, Langenecker SA, Jacobs RH. Aberrant resting-state functional connectivity in limbic and cognitive control networks relates to depressive rumination and mindfulness: A pilot study among adolescents with a history of depression. J Affect Disord. 2016;200: 178–181.

51. Gerlach AR, Karim HT, Kolobaric A, Boyd BD, Kahru K, Krafty RT, et al. Network homeostasis: functional brain network alterations and relapse in remitted late-life depression. Neuropsychopharmacology. 2025;50: 1493–1501.

52. Moliner R, Girych M, Brunello CA, Kovaleva V, Biojone C, Enkavi G, et al. Psychedelics promote plasticity by directly binding to BDNF receptor TrkB. Nat Neurosci. 2023;26: 1032–1041.

53. Li N, Lee B, Liu R-J, Banasr M, Dwyer JM, Iwata M, et al. mTOR-dependent synapse formation underlies the rapid antidepressant effects of NMDA antagonists. Science. 2010;329: 959–964.

54. Yang C, Ren Q, Qu Y, Zhang J-C, Ma M, Dong C, et al. Mechanistic Target of Rapamycin-Independent Antidepressant Effects of (R)-Ketamine in a Social Defeat Stress Model. Biol Psychiatry. 2018;83: 18–28.

55. Carrier N, Kabbaj M. Sex differences in the antidepressant-like effects of ketamine. Neuropharmacology. 2013;70: 27–34.

56. Yang C, Hu Y-M, Zhou Z-Q, Zhang G-F, Yang J-J. Acute administration of ketamine in rats increases hippocampal BDNF and mTOR levels during forced swimming test. Ups J Med Sci. 2013;118: 3–8.

57. Miller OH, Yang L, Wang C-C, Hargroder EA, Zhang Y, Delpire E, et al. GluN2B-containing NMDA receptors regulate depression-like behavior and are critical for the rapid antidepressant actions of ketamine. Elife. 2014;3: e03581.

58. Zhou W, Wang N, Yang C, Li X-M, Zhou Z-Q, Yang J-J. Ketamine-induced antidepressant effects are associated with AMPA receptors-mediated upregulation of mTOR and BDNF in rat hippocampus and

prefrontal cortex. Eur Psychiatry. 2014;29: 419–423.

59. Holubova K, Kleteckova L, Skurlova M, Ricny J, Stuchlik A, Vales K. Rapamycin blocks the antidepressant effect of ketamine in task-dependent manner. Psychopharmacology (Berl). 2016;233: 2077–2097.

60. Paul RK, Singh NS, Khadeer M, Moaddel R, Sanghvi M, Green CE, et al. (R,S)-Ketamine metabolites (R,S)-norketamine and (2S,6S)-hydroxynorketamine increase the mammalian target of rapamycin function. Anesthesiology. 2014;121: 149–159.

61. Zhang K, Yamaki VN, Wei Z, Zheng Y, Cai X. Differential regulation of GluA1 expression by ketamine and memantine. Behav Brain Res. 2017;316: 152–159.

62. Zanos P, Gould TD. Mechanisms of ketamine action as an antidepressant. Mol Psychiatry. 2018;23: 801–811.

63. Duman RS, Li N, Liu R-J, Duric V, Aghajanian G. Signaling pathways underlying the rapid antidepressant actions of ketamine. Neuropharmacology. 2012;62: 35–41.

64. Kang MJY, Hawken E, Vazquez GH. The Mechanisms Behind Rapid Antidepressant Effects of Ketamine: A Systematic Review With a Focus on Molecular Neuroplasticity. Front Psychiatry. 2022;13: 860882.

65. Voleti B, Navarria A, Liu R-J, Banasr M, Li N, Terwilliger R, et al. Scopolamine rapidly increases mammalian target of rapamycin complex 1 signaling, synaptogenesis, and antidepressant behavioral responses. Biol Psychiatry. 2013;74: 742–749.

66. Liu X-L, Luo L, Mu R-H, Liu B-B, Geng D, Liu Q, et al. Fluoxetine regulates mTOR signalling in a region-dependent manner in depression-like mice. Sci Rep. 2015;5: 16024.

67. Xu D, Wang C, Zhu X, Zhao W, Jiang B, Cui S, et al. The antidepressant-like effects of fluvoxamine in mice involve the mTOR signaling in the hippocampus and prefrontal cortex. Psychiatry Res. 2020;285: 112708.

68. Park SW, Lee JG, Seo MK, Lee CH, Cho HY, Lee BJ, et al. Differential effects of antidepressant drugs on mTOR signalling in rat hippocampal neurons. Int J Neuropsychopharmacol. 2014;17: 1831–1846.

69. Koike H, Iijima M, Chaki S. Involvement of the mammalian target of rapamycin signaling in the antidepressant-like effect of group II metabotropic glutamate receptor antagonists. Neuropharmacology. 2011;61: 1419–1423.

70. Zhou Q, Dong J, Xu T, Cai X. Synaptic potentiation mediated by L-type voltage-dependent calcium channels mediates the antidepressive effects of lateral habenula stimulation. Neuroscience. 2017;362: 25–32.

71. Hoeffer CA, Klann E. mTOR signaling: at the crossroads of plasticity, memory and disease. Trends Neurosci. 2010;33: 67–75.

72. Hay N, Sonenberg N. Upstream and downstream of mTOR. Genes Dev. 2004;18: 1926–1945.

73. Klann E, Dever TE. Biochemical mechanisms for translational regulation in synaptic plasticity. Nat Rev Neurosci. 2004;5: 931–942.

74. Jernigan CS, Goswami DB, Austin MC, Iyo AH, Chandran A, Stockmeier CA, et al. The mTOR signaling pathway in the prefrontal cortex is compromised in major depressive disorder. Prog Neuropsychopharmacol Biol Psychiatry. 2011;35: 1774–1779.

75. Müller MB, Toschi N, Kresse AE, Post A, Keck ME. Long-term repetitive transcranial magnetic stimulation increases the expression of brain-derived neurotrophic factor and cholecystokinin mRNA, but not neuropeptide tyrosine mRNA in specific areas of rat brain. Neuropsychopharmacology. 2000;23: 205–215.

76. Podda MV, Cocco S, Mastrodonato A, Fusco S, Leone L, Barbati SA, et al. Anodal transcranial direct current stimulation boosts synaptic plasticity and memory in mice via epigenetic regulation of Bdnf expression. Sci Rep. 2016;6: 22180.

77. Wang H-Y, Crupi D, Liu J, Stucky A, Cruciata G, Di Rocco A, et al. Repetitive transcranial magnetic stimulation enhances BDNF-TrkB signaling in both brain and lymphocyte. J Neurosci. 2011;31: 11044–11054.

78. Hamani C, Machado DC, Hipólide DC, Dubiela FP, Suchecki D, Macedo CE, et al. Deep brain stimulation reverses anhedonic-like behavior in a chronic model of depression: role of serotonin and brain derived neurotrophic factor. Biol Psychiatry. 2012;71: 30–35.

79. Bambico FR, Bregman T, Diwan M, Li J, Darvish-Ghane S, Li Z, et al. Neuroplasticity-dependent and -independent mechanisms of chronic deep brain stimulation in stressed rats. Transl Psychiatry. 2015;5: e674.

80. Zanardini R, Gazzoli A, Ventriglia M, Perez J, Bignotti S, Rossini PM, et al. Effect of repetitive transcranial magnetic stimulation on serum brain derived neurotrophic factor in drug resistant depressed patients. J Affect Disord. 2006;91: 83–86.

81. Yukimasa T, Yoshimura R, Tamagawa A, Uozumi T, Shinkai K, Ueda N, et al. High-frequency repetitive transcranial magnetic stimulation improves refractory depression by influencing catecholamine and brain-derived neurotrophic factors. Pharmacopsychiatry. 2006;39: 52–59.

82. Ma J, Zhang Z, Su Y, Kang L, Geng D, Wang Y, et al. Magnetic stimulation modulates structural synaptic plasticity and regulates BDNF-TrkB signal pathway in cultured hippocampal neurons. Neurochem Int. 2013;62: 84–91.

83. Johnson SC, Rabinovitch PS, Kaeberlein M. mTOR is a key modulator of ageing and age-related disease. Nature. 2013;493: 338–345.

84. Yang S-B, Tien A-C, Boddupalli G, Xu AW, Jan YN, Jan LY. Rapamycin ameliorates age-dependent obesity associated with increased mTOR signaling in hypothalamic POMC neurons. Neuron. 2012;75: 425–436.

85. Wilkinson JE, Burmeister L, Brooks SV, Chan C-C, Friedline S, Harrison DE, et al. Rapamycin slows aging in mice. Aging Cell. 2012;11: 675–682.

86. Caccamo A, Magrì A, Medina DX, Wisely EV, López-Aranda MF, Silva AJ, et al. mTOR regulates tau phosphorylation and degradation: implications for Alzheimer's disease and other tauopathies. Aging Cell. 2013;12: 370–380.

87. Mohallem R, Schaser AJ, Aryal UK. Molecular Signatures of Neurodegenerative Diseases Identified by Proteomic and Phosphoproteomic Analyses in Aging Mouse Brain. Mol Cell Proteomics. 2024;23: 100819.

88. Baar EL, Carbajal KA, Ong IM, Lamming DW. Sex- and tissue-specific changes in mTOR signaling with age in C57BL/6J mice. Aging Cell. 2016;15: 155–166.

89. Miller RA, Harrison DE, Astle CM, Fernandez E, Flurkey K, Han M, et al. Rapamycin-mediated lifespan increase in mice is dose and sex dependent and metabolically distinct from dietary restriction. Aging Cell. 2014;13: 468–477.

90. Balmer TS. Perineuronal Nets Enhance the Excitability of Fast-Spiking Neurons. eNeuro. 2016;3. doi:10.1523/ENEURO.0112-16.2016

91. Wingert JC, Sorg BA. Impact of Perineuronal Nets on Electrophysiology of Parvalbumin Interneurons, Principal Neurons, and Brain Oscillations: A Review. Front Synaptic Neurosci. 2021;13: 673210.

92. Sigal YM, Bae H, Bogart LJ, Hensch TK, Zhuang X. Structural maturation of cortical perineuronal nets and their perforating synapses revealed by superresolution imaging. Proc Natl Acad Sci U S A. 2019;116: 7071–7076.

93. Fawcett JW, Oohashi T, Pizzorusso T. The roles of perineuronal nets and the perinodal extracellular matrix in neuronal function. Nat Rev Neurosci. 2019;20: 451–465.

94. Murthy S, Kane GA, Katchur NJ, Lara Mejia PS, Obiofuma G, Buschman TJ, et al. Perineuronal Nets, Inhibitory Interneurons, and Anxiety-Related Ventral Hippocampal Neuronal Oscillations Are Altered by Early Life Adversity. Biol Psychiatry. 2019;85: 1011–1020.

95. Belliveau C, Rahimian R, Fakhfouri G, Hosdey C, Simard S, Davoli MA, et al. Evidence of microglial involvement in the childhood abuse-associated increase in perineuronal nets in the ventromedial prefrontal cortex. Brain Behav Immun. 2025;124: 321–334.

96. Thompson EH, Lensjø KK, Wigestrand MB, Malthe-Sørenssen A, Hafting T, Fyhn M. Removal of perineuronal nets disrupts recall of a remote fear memory. Proc Natl Acad Sci U S A. 2018;115: 607–612.

97. Mehak SF, Shivakumar AB, Jijimon F, Gupta A, Pillai VG, Gangadharan G. Targeting CA2 Perineuronal Nets Restores Recognition Memory and Theta Oscillations in Aged Mice. Aging Cell. 2025; e70139.

98. Tarakcioglu E, Genc B, Tufekci KU, Genc S. Neonatal NLRP3 Inflammasome Activation Leads to Perineuronal Net Deficits in Early Adulthood. Dev Neurobiol. 2025;85: e22986.

99. Benacom D, Chataing C, Prochiantz A, Di Nardo AA. Motor recovery through perineuronal net modulation in a Parkinson's disease mouse model. Brain. 2025. doi:10.1093/brain/awaf226

100. de Vries LE, Bahnerth A, Swaab DF, Verhaagen J, Carulli D. Resilience to Alzheimer's disease associates with alterations in perineuronal nets. Alzheimers Dement. 2025;21: e14504.

101. Matuszko G, Curreli S, Kaushik R, Becker A, Dityatev A. Extracellular matrix alterations in the ketamine model of schizophrenia. Neuroscience. 2017;350: 13–22.

102. Kaushik R, Lipachev N, Matuszko G, Kochneva A, Dvoeglazova A, Becker A, et al. Fine structure analysis of perineuronal nets in the ketamine model of schizophrenia. Eur J Neurosci. 2021;53: 3988–4004.

103. Huang A, Chen Y, Wang S, Du H, Guan A, Wu H, et al. Esketamine ameliorates post-stroke anxiety by modulating microglial HDAC3/NF-κB/COX1 inflammatory signaling in ischemic cortex. Eur J Pharmacol. 2023;947: 175667.

104. Robinson PK, Jarome TJ, Trask S. Differential impacts of advanced age and sex in age-related trace fear memory impairment in rats. Learn Mem. 2025;32. doi:10.1101/lm.054159.125

105. Tanaka Y, Mizoguchi K. Influence of aging on chondroitin sulfate proteoglycan expression and neural stem/progenitor cells in rat brain and improving effects of a herbal medicine, yokukansan. Neuroscience. 2009;164: 1224–1234.

106. Karetko-Sysa M, Skangiel-Kramska J, Nowicka D. Aging somatosensory cortex displays increased density of WFA-binding perineuronal nets associated with GAD-negative neurons. Neuroscience. 2014;277: 734–746.

107. Yamada J, Jinno S. Spatio-temporal differences in perineuronal net expression in the mouse hippocampus, with reference to parvalbumin. Neuroscience. 2013;253: 368–379.

108. Gildawie KR, Honeycutt JA, Brenhouse HC. Region-specific Effects of Maternal Separation on Perineuronal Net and Parvalbumin-expressing Interneuron Formation in Male and Female Rats. Neuroscience. 2020;428: 23–37.

109. Foscarin S, Raha-Chowdhury R, Fawcett JW, Kwok JCF. Brain ageing changes proteoglycan sulfation, rendering perineuronal nets more inhibitory. Aging (Albany NY). 2017;9: 1607–1622.

110. Yamada J, Ohgomori T, Jinno S. Alterations in expression of Cat-315 epitope of perineuronal nets during normal ageing, and its modulation by an open-channel NMDA receptor blocker, memantine. J Comp Neurol. 2017;525: 2035–2049.

111. Drzewiecki CM, Willing J, Juraska JM. Influences of age and pubertal status on number and intensity of perineuronal nets in the rat medial prefrontal cortex. Brain Struct Funct. 2020;225: 2495–2507.

112. Laham BJ, Murthy SS, Hanani M, Clappier M, Boyer S, Vasquez B, et al. The estrous cycle modulates early-life adversity effects on mouse avoidance behavior through progesterone signaling. Nat Commun. 2022;13: 7537.

113. Hernández-Vivanco A, Cano-Adamuz N, Sánchez-Aguilera A, González-Alonso A, Rodríguez-Fernández A, Azcoitia Í, et al. Sex-specific regulation of inhibition and network activity by local aromatase in the mouse hippocampus. Nat Commun. 2022;13: 3913.

114. Nguyen R, Rahyab R, Deshpande A, Legge E, Almeida J, Herz SM, et al. Estrogenic regulation of perineuronal nets in the mouse insular cortex and hippocampus. Neuropharmacology. 2025;279: 110641.

115. Santos-Silva T, Souza BK, Colodete DAE, Campos LR, Lima TSA, Guimarães FS, et al. Differential Impact of Adolescent or Adult Stress on Behavior and Cortical Parvalbumin Interneurons and Perineuronal Nets in Male and Female Mice. Int J Neuropsychopharmacol. 2024;27. doi:10.1093/ijnp/pyae042

116. Page CE, Coutellier L. Adolescent Stress Disrupts the Maturation of Anxiety-related Behaviors and Alters the Developmental Trajectory of the Prefrontal Cortex in a Sex- and Age-specific Manner. Neuroscience. 2018;390: 265–277.